ACS APPLIED MATERIALS & INTERFACES

Research Article

Cite This: ACS Appl. Mater. Interfaces 2018, 10, 27160−27170

www.acsami.org

Microwave-Assisted Heating Method toward Multicolor Quantum Dot-Based Phosphors with Much Improved Luminescence

Ding Zhou,[†] Yi Wang,[‡] Pengfei Tian,[§] Pengtao Jing,[†] Maolei Sun,[∥] Xi Chen,[∥] Xiaowei Xu,*[,∥] Di Li,[†] Shiliang Mei,[§] Xiaoyan Liu,[§] Wanlu Zhang,[§] Ruiqian Guo,*[,§] Songnan Qu,*[,†] and Hao Zhang*[,⊥]

[†]State Key Laboratory of Luminescence and Applications, Changchun Institute of Optics, Fine Mechanics and Physics, Chinese Academy of Sciences, Changchun 130033, P. R. China

[‡]College of Physics and [⊥]State Key Laboratory of Supramolecular Structure and Materials, College of Chemistry, Jilin University, Changchun 130012, P. R. China

[§]Engineering Research Center of Advanced Lighting Technology, Ministry of Education; Institute for Electric Light Sources, Fudan University, Shanghai 200433, P. R. China

[∥]Department of Periodontology, School and Hospital of Stomatology, Jilin University, Changchun 130021, P. R. China

Supporting Information

ABSTRACT: Solid-state highly photoluminescent quantum dot (QD)-based phosphors attract great scientific interests as color converters because of an increasing demand for white-light-emitting devices. Herein, a microwave-assisted heating method is presented to fabricate multicolor QD-based phosphors within 30 s through microwave-assisted heating of the mixture of QDs and sodium silicate aqueous solution. In the composites, the formed cross-linked networks not only play as a matrix to prevent QD aggregation in solid state but also cause the variation of the refractive index around QDs and the QD surface optimization, which contributes to good stabilities and twice enhancement in photoluminescence quantum yields (69%) compared with the initial QD aqueous solution (33%). Using the QD-based phosphors as color conversion layers, white-light-emitting diodes were realized with controllable color temperature, high color purity, and high color-rendering index (90.3), which show a great potential in display and illumination. Furthermore, the luminescence lifetime of the QD-based phosphors is less than 25 ns. The potential application of the QD-based phosphors in visible light communication was also demonstrated, with the modulation bandwidth achieving 42 MHz.

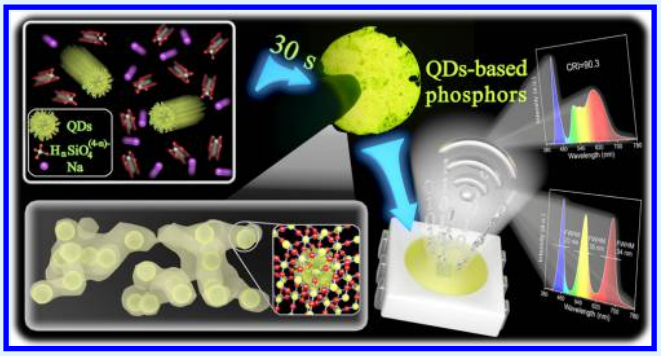

KEYWORDS: *aqueous quantum dot, sodium silicate, phosphors, white-light-emitting diode, visible light communication*

Solid-state lighting made of compound semiconductor materials has sparked the third lighting revolution in the history of lighting industry[1] and promoted the improvement of energy efficiency.[2] In particular, the presence of white-light-emitting diodes (WLEDs) has intrigued lots of research for extensive applications in illumination and display.[3] In general, the commercial WLEDs are composed of a InGaN chip with blue emission and some phosphors,[4] where the phosphors can convert the blue light into other colors and are very crucial to the parameters of WLEDs, such as Commission Internationale de l'Eclairage (CIE) chromaticity coordinate, correlated color temperature (CCT), color-rendering index (CRI), and luminous efficacy. Besides illumination and display, wireless data communication based on LEDs, also known as visible light communication (VLC), has attracted growing attentions.[5] After Komine and Nakagawa suggested the thought of combining illumination and data communication in one LED in 2003,[6] numerous work on VLC has been proposed.[7−9] Because of the intense and inconstant research following the originated work, it becomes an urge to set a standard for researchers worldwide. Such a standard of VLC was released by IEEE in 2011 eventually. Although a standard has been released, usage of VLC still meet various challenges, such as increasing data rate, provision of an uplink, and regulatory challenges.[10] With respect to the current broadband radio frequency (used by traditional Wi-Fi)/microwave wireless technologies, VLC has shown great potential in realizing fast wireless data communication because of its theoretically higher bandwidth, but it also brings up higher requirements for the phosphors.[7] Currently, commercial and wildly used phosphors for WLEDs are usually rare-earth phosphors, whereas their relatively long luminescence lifetimes restrict their perform-

Received: April 18, 2018
Accepted: July 26, 2018
Published: July 26, 2018

DOI: 10.1021/acsami.8b06323
ACS Appl. Mater. Interfaces 2018, 10, 27160−27170

ance in VLC.[8,9,11−13] The bandwidth of VLC based on rare-earth phosphors is usually less than 12 MHz.[14] Although laser-based VLC with multiple GHz is proposed,[10] their low CRI and high cost are not favorable for illumination in the practical application. Furthermore, the low reserves and nonrenewability of rare-earth phosphors on the earth would lead to the concerns of environmental destruction.[15] Therefore, alternative solid-state luminescent materials for color conversion layer are strongly desirable for the improvement of the quality of WLEDs and the promotion for their developments in VLC.

Inorganic quantum dots (QDs) show high competition ability acting as color conversion layer for illumination,[16] display,[17] and VLC[18] because of tunable and narrow photoluminescence (PL),[19−29] high PL quantum yields (PLQYs),[30−36] good photostability,[37−41] broad excitation spectra,[42−46] and short luminescence lifetime.[18] In particular, aqueous synthesis of QDs is facile and close to the green chemistry concept compared with those prepared in organic media,[47−49] such as oil-soluble semiconductor QDs and perovskite QDs. Moreover, aqueous QDs possess much better stability with respect to perovskite QDs. In the long-term preservation, the anion-exchange reaction could bring about serious deterioration to the PL property of perovskite QDs.[50] Nevertheless, PL emission of water-soluble QDs can be severely quenched in the solid state.[51] To address this issue, several approaches have been proposed for fabricating QD-based solid-state composites.[30,52−58] In spite of the achievements of these approaches in constructing QD-based composites, these synthesis processes are difficult to satisfy the requirements of both high luminescence and quick synthesis in large quantity. Therefore, it is an urgent need to exploit more effective methods for the preparation of QD-based phosphors with high PLQYs.

Highly luminescent aqueous QDs can be obtained at room temperature by simply adding reagents in one pot stepwise, as reported in our previous research, which is favorable for mass production.[59] Herein, we proposed a preparation route for multicolor QD-based phosphors through microwave-assisted heating of the mixture of QDs and sodium silicate aqueous solution within only 30 s. The as-prepared QD-based phosphors possess more than twice the enhancement in PLQYs compared with the initial QD aqueous solutions, which should be ascribed to the variation of the refractive index around QDs and the QD surface optimization. Additionally, the QD-based phosphors own narrow PL emission, good photostability, thermal, solvent, and mechanical stability. Modulating multiple different emissive QD-based phosphors, WLEDs with high color purity, controllable CCT, and high CRI (90.3) were achieved. Furthermore, because of the short luminescence lifetime (<25 ns) of the phosphors, a VLC prototype with a modulation bandwidth of 42 MHz was realized.

RESULTS AND DISCUSSION

Aqueous CdTe QDs decorated by 3-mercaptopropionic acid (MPA) are prepared, as described in the Methods section.[59] After adding the reagents in one pot, the QD solution is stored at room temperature in air under atmospheric pressure. By altering the storage durations from 1, 3, 8, 16, to 30 h, QDs with emissions of 520, 560, 590, 620, and 660 nm are formed (Figure S1). To terminate the QD growth, 2-propanol is added into QD solution to remove $N_2H_4{\cdot}H_2O$, and the mixture solution is centrifuged. Afterward, the resultant precipitates are dissolved in aqueous solution. The aqueous solution contains cadmium chloride and MPA, and its pH is adjusted to 9.5 before use. All of the full width at half maximum (fwhm) of these solutions are less than 50 nm (Figure S1). The wide range of emission colors and narrow PL emission peaks ensure excellent CRI for illumination and the high color purity for tricolor display. The as-prepared CdTe QDs display a regular crystalline structure in consistence with the zinc blende structure (Figure S2a), in confirmation with X-ray powder diffraction pattern (Figure S2b).[59] Because there are abundant carboxyl groups on QD surface, the as-prepared CdTe QDs could be well-dissolved in hydrophilic solvents. $Na_2SiO_3{\cdot}9H_2O$ aqueous solution, also known as liquid glass, could dehydrate and solidify fast during the microwave-assisted heating process, resulting in solid-state glass-like structures,[60] and their low cost and low toxicity make them more competitive candidates among various matrix materials. In particular, the alkalinity of $Na_2SiO_3{\cdot}9H_2O$ aqueous solution can deprotonate the carboxylic groups of MPA,[60] thus providing an electrostatic repulsive force for the stabilization of QDs. Therefore, QDs and $Na_2SiO_3{\cdot}9H_2O$ aqueous solution can form a homogeneous and stabilized mixed solution, ensuring the following preparation of QD-based phosphors.

QD-based phosphors are synthesized through microwave-assisted heating CdTe QDs and sodium silicate aqueous solution together within 30 s, during which CdTe QDs are rapidly encapsulated in situ (Figure 1). No further filtration,

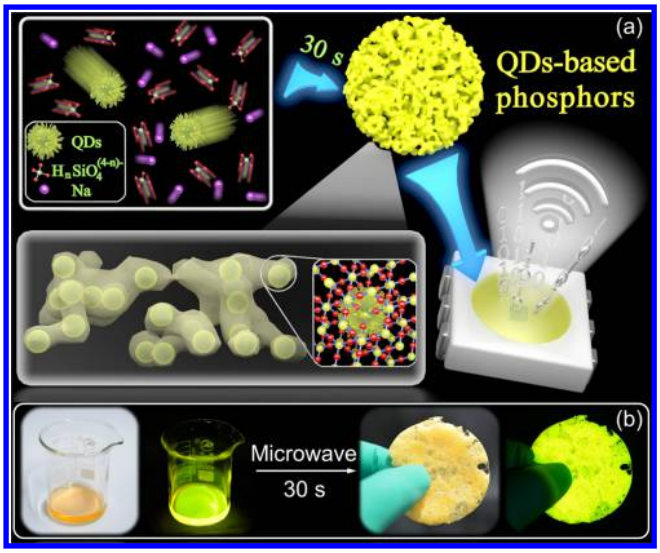

Figure 1. (a) Schematics and (b) photographic illustration of the microwave-assisted heating method for QD-based phosphors.

rinsing, and drying are needed, leading to less cost and time consumption compared with other preparation methods.[61] As shown in Figure 2a,b, the QD-based phosphors can be mass-produced at one time, and the PL images demonstrate bright emission of the phosphors. By using different emissive QDs, the QD-based phosphors with different emission colors could be achieved, covering the emission range from 520 to 660 nm (Figure 2c). Compared with the PL emission of the initial QD aqueous solutions, there are nearly no red shift in the PL spectra of the phosphors (Figure S1 and Table 1). This is mainly because of the rapid dehydration process, where QDs are encapsulated in situ in this short time without aggregating, thus retaining good monodispersity in the matrix.[37] The

DOI: 10.1021/acsami.8b06323
ACS Appl. Mater. Interfaces 2018, 10, 27160−27170

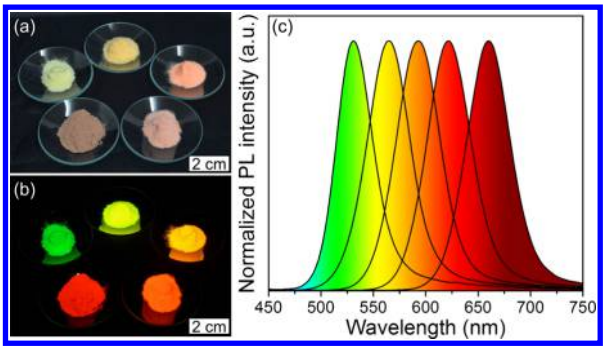

Figure 2. (a) Optical and (b) PL images of the CdTe QD-based phosphors with different emissions. (c) Corresponding emission spectra of the phosphors.

narrow fwhm (<50 nm) of the QD-based phosphors also indicate the well-monodispersed QDs in the matrix (Figure 2c and Table 1). Under UV light excitation, the phosphors possess homogeneous luminescence (Figure S3), implying that the QDs are distributed well in matrix.

To further characterize the structure and composition of the QD-based phosphors, high-resolution transmission electron microscopy (HRTEM), energy-dispersive spectroscopy (EDS), scanning electron microscopy (SEM) studies, and Fourier transform infrared (FTIR) characterizations are carried out. Under HRTEM observation, the 0.37 nm lattice spacing of QDs can be observed (Figure 3a), which is consistent with the (111) lattice planes of bulk CdTe crystal (Figure S2).[59] It is clearly observed that in the phosphors, CdTe QDs are in good distribution. In contrast, the powders of pure CdTe QDs, which are obtained through adding 2-propanol into QDs solution, present obvious aggregation (Figure S4). Under HRTEM observation, the matrix surrounding QDs has no obvious lattice, indicating the amorphous structure of the matrix. The matrix is originating from the rapid dehydration process of adjacent silanol groups (Si−OH) in $Na_2SiO_3{\cdot}9H_2O$ aqueous solution (Figures 1a and S4), leading to silicon oxide network structure through the Si−O−Si bond formation.[60] EDS confirms the presence of cadmium and tellurium, indicating that CdTe QDs are incorporated into phosphors (Figure 3b). By altering the concentration of the initial QD aqueous solution, the loading fraction of QDs in phosphors could be facilely tuned from 0 to 15 wt %. SEM image reveals a 3D cross-linked architecture (Figure 3c), which is originated from the rapid dehydration process of $Na_2SiO_3{\cdot}9H_2O$ aqueous solution (explanatory text in the Supporting Information). Besides the cross-linking of $Na_2SiO_3{\cdot}9H_2O$ itself, because there are plentiful carboxyl on QD surface, the dehydration processes involve not only the Si−OH groups but also the carboxyl on QDs surface (Figure 3e and explanatory text in the Supporting Information). FTIR characterizations are carried out for demonstrating the chemical cross-linking between QDs and the matrix. The FTIR spectrum of CdTe QDs decorated by MPA presents a sharp peak at 1700 cm^{-1} and a broad peak at 2600−3300 cm^{-1}, which are assigned to $\nu_{(C=O)}$ and $\nu_{(O-H)}$, respectively. In QD-based phosphors, the O−H stretching disappears because of the dehydration between the Si−OH groups and the carboxyl on QD surface. In addition, $\nu_{(C=O)}$ shifts to 1750 cm^{-1}, which is assigned to O═C−O−Si. All of these results indicate the presence of chemical cross-linking between QDs and the matrix. Then, the QD-based phosphors are grinded carefully into powders for subsequent applications in LEDs. SEM image of the resultant powders present spherical particles with size from 30 to 200 nm (Figure 3d), and their PL spectrum and PLQYs (65%) have no variations after grinding (Figure S5). When these powders are mixed with various packaging materials for LEDs, their spherical structure and small size provide many advantages, including good slurry properties, high packing densities, and smooth light-intensity distributions.[62] More importantly, together with physical encapsulation, there are chemical cross-linking between QDs and the matrix; therefore, it should be of benefit to passivate QDs by saturating the surface-dangling bonds, therewith optimizing the PL properties and enhancing the stability of QDs.

To demonstrate our supposition, absolute PLQYs of the initial CdTe QD aqueous solutions and QD-based phosphors are investigated (Table 1). As indicated in Table 1, all QD-based phosphors possess higher PLQYs than that of the corresponding initial QD aqueous solutions. The highest PLQYs could reach 69% (Table 1). The observed PLQY enhancement can be understood in terms of two factors: the effects of the refractive index of the ambient environment (i.e., dielectric surrounding) and the passivation of QD surface. It is from the Strickler−Berg equation that we can figure out the effect of refractive index on PLQYs.[42]

$$k_r(\bar{n}) = \bar{n}^2 \cdot k_{rv} \quad (1)$$

where k_r represents the radiative rate constant of luminescent species when being encapsulated by a surrounding material, $\bar{n}$ represents the refractive index of the surrounding material, and k_{rv} is the radiative rate constant of luminescent species under vacuum. Because the refractive indices of water and cross-

Table 1. Comparison of PL Emission, Absolute PLQYs, fwhm, and Lifetime of CdTe QD Aqueous Solutions and the Corresponding CdTe QD-Based Phosphors, PLQY Enhancement Factor ($(\Phi_{phosphores} - \Phi_{solution})/\Phi_{solution}$), and PLQY Enhancement Calculated by Strickler−Berg Equation

aqueous CdTe QDs	PL emission (nm)	526	562	591	620	660
	absolute PLQYs (%)	15	33	29	25	22
	fwhm (nm)	36	44	49	49	49
	lifetime (ns)	9.6	19.4	17.1	15.8	10.1
QDs-based phosphors	PL emission (nm)	528	565	593	621	660
	absolute PLQYs (%)	29	69	62	52	48
	fwhm (nm)	37	45	49	49	49
	lifetime (ns)	11.3	24.2	20.2	17.4	13.1
PLQYs enhancement factor (%)		93.3	109.1	113.8	108.1	118.2
PLQYs enhancement calculated by Strickler−Berg equation (%)		51.5	36.6	39.6	42.8	45.3

DOI: 10.1021/acsami.8b06323
ACS Appl. Mater. Interfaces 2018, 10, 27160−27170

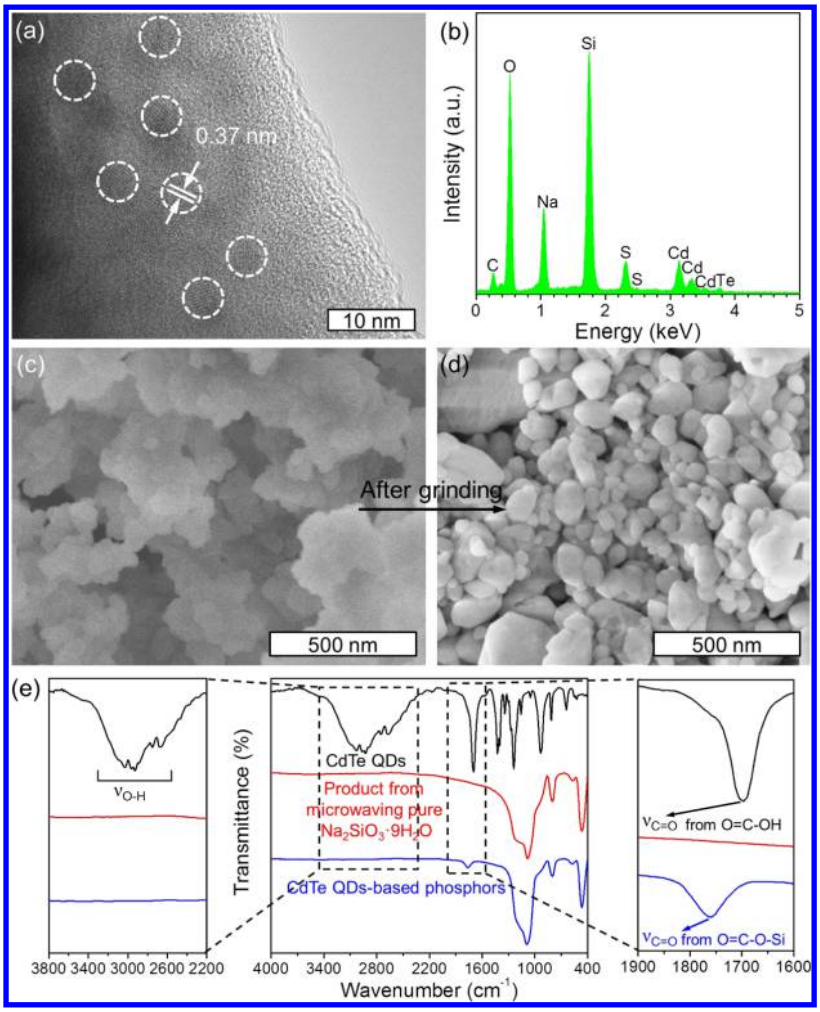

Figure 3. (a) HRTEM image and (b) EDS pattern of CdTe QD-based phosphors. (c,d) SEM images of CdTe QD-based phosphors (c) before and (d) after grinding. (e) FTIR characterizations of CdTe QDs (black line), a product from microwaving pure $Na_2SiO_3 \cdot 9H_2O$ solution (red line), and CdTe QD-based phosphors (blue line).

linked silicon oxide are 1.33 and 1.47, respectively,[63] the enhancement of radiative rate constant of QDs in silicon oxide matrix could be up to 25% compared with QDs in water. From the equation of PLQYs [$\Phi = k_r/(k_r + k_{nr})$, where k_{nr} represents the nonradiative rate constant], PLQYs can be enhanced up to about 35−50% according to calculations. Additionally, CdTe possesses a much higher refractive index of 2.87.[63] The large difference in refractive index between CdTe and water would lead to a small critical angle of total internal reflection on the QDs−water interface, causing light to reflect back into QDs at normal incidence.[64] In contrast to water, the higher refractive index of cross-linked silicon oxide could reduce the total internal reflection, enhancing light-extraction efficiency and therewith PLQYs.[64]

However, in this work, the actual PLQYs enhancement factor $[(\Phi_{phosphores} - \Phi_{solution})/\Phi_{solution}]$ is ca. 100%, which exceeds the PL enhancement brought by the influence of refractive index (Table 1). Therefore, the passivation of CdTe QD surface by the cross-linked structure should be another significant attribute to higher PLQYs.[16] To gain a detailed understanding, femtosecond transient absorption (TA) spectroscopic measurements of CdTe QD aqueous solution and the corresponding QD-based phosphors, whose absorption peaks are located at 520 nm, are carried out under magic angle polarization configurations with an excitation of 400 nm at 10 μW, as presented in Figure 4. There is an obvious ground-state bleaching (GSB) band centered at 520 nm (Figure 4a,d), which represents a depopulation channel for electrons in excited states. The decay of GSB process of QD aqueous solution seems faster than that of the QD-based phosphors. To prove this, TA kinetic traces probed at 520 nm are sketched to analyze the temporal evolution of electrons in excited states (Figure 4b,e). It is found that there is a fast relaxation process from 1 to 3 ps in both spectra, suggesting the existence of nonradiative recombination, whereas the nonradiative recombination rates of charge carriers are obviously decreased in the QD-based phosphors (Figure 4b,e). This demonstrates the optimization of QD surface through saturating the surface dangling bonds (Figure 3e), which contributes to the decrease of surface traps and therewith the increase of PLQYs. PL decay curves (375 nm excitation) are further measured (Figure 4c,f). The average PL lifetimes of CdTe QDs solutions are 9.6, 19.4, 17.1, 15.8, and 10.1 ns, respectively (Table 1). When incorporating QDs into phosphors, the PL lifetimes are accordingly extended to 11.3, 24.2, 20.2, 17.4, and 13.1 ns, respectively (Table 1), which demonstrates the decrease of energy losses in the phosphors in comparison with their initial QD aqueous solutions, resulting in the PLQY enhancement.

DOI: 10.1021/acsami.8b06323
ACS Appl. Mater. Interfaces 2018, 10, 27160−27170

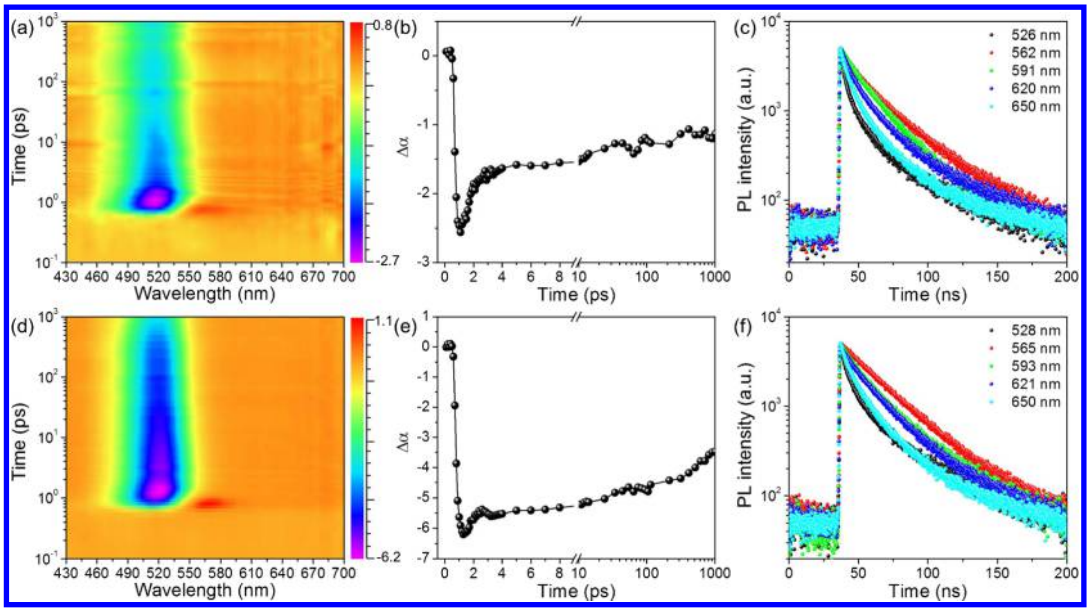

Figure 4. Top-view TA spectra of (a) CdTe QDs solution and (d) corresponding CdTe QD-based phosphors under magic-angle polarization configurations with excitation of 400 nm at 10 μW. TA kinetic traces of (b) CdTe QD aqueous solution and (e) corresponding CdTe QD-based phosphors probed at 520 nm. Time-resolved PL decay curves of different emissive (c) CdTe QD aqueous solutions and (f) corresponding phosphors collected at individual PL peak positions.

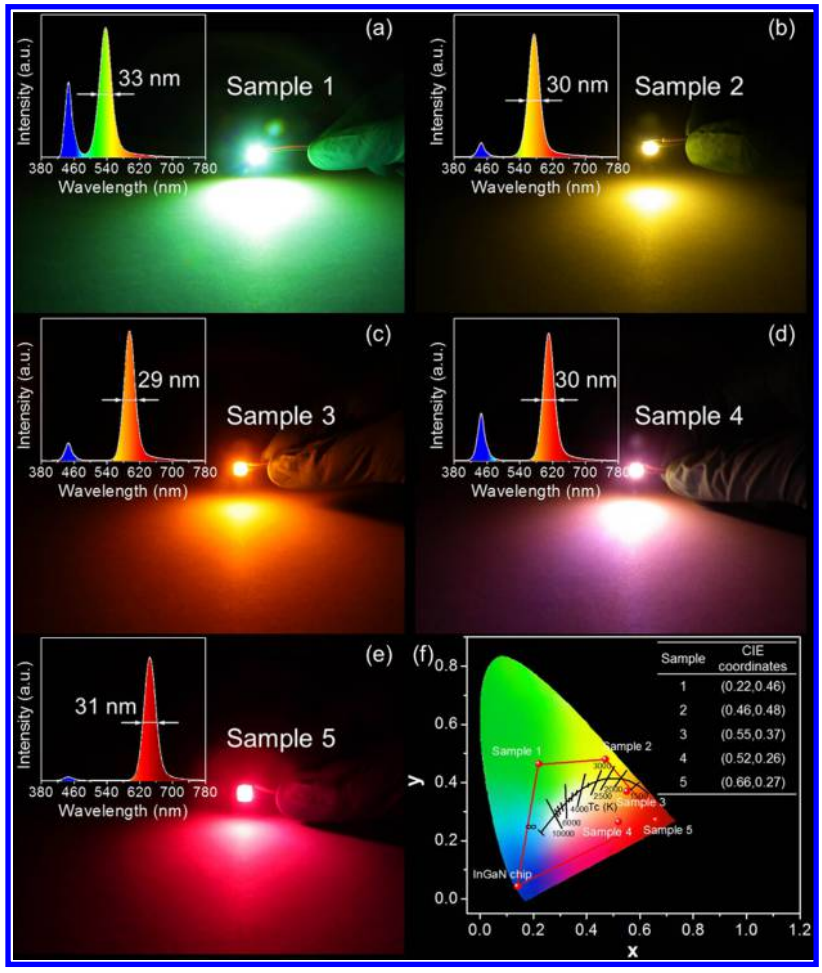

Figure 5. LED prototypes with (a) green, (b) yellow, (c) orange, (d) pink, and (e) red emission. Insets in (a–e) are the emission spectra of LEDs. (f) CIE chromaticity diagram showing the CIE color coordinates of the five LED lights. The black curve stands for the variety of CCT with respect to the CIE color coordinate. The points on the black straight line represent constant CCT.

DOI: 10.1021/acsami.8b06323
ACS Appl. Mater. Interfaces 2018, 10, 27160–27170

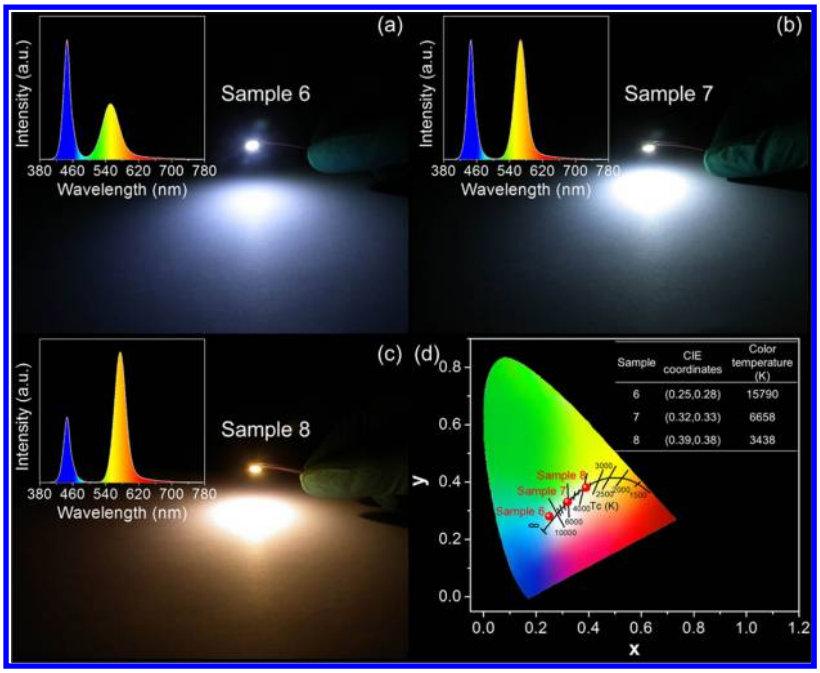

Figure 6. (a–c) Photographs of three working WLEDs with different CCT. The insets of (a–c) are the corresponding emission spectra. (d) CIE color coordinates of WLEDs are also shown.

To conclude, two reasons cause the PLQY enhancement: the variation of the refractive index around QDs and the QD surface optimization.

Owing to the protection of the cross-linked structure, the QD-based phosphors present good resistance against sunlight. We also testified the photostability of phosphors, which is revealed by variations in the PL spectra during 3 months sunlight irradiation in air (Figure S6). It is found that there are nearly no changes in PL spectra and PLQYs. However, for the aqueous CdTe QDs, the PL emission peak has an obvious blue shift, and the intensity presents a serious reduction during 3 days' sun exposure, suggesting the decomposition of QDs. Along with good photostability, good thermal stability is also indicated. PL spectra of the QD-based phosphors are measured and supplied before and after a 100 °C thermal treatment for 2 h (Figure S7), where the testing temperature is higher than the curing temperature (80 °C) for the LED packaging process. No apparent variations in the spectra indicate the good thermal stability. Furthermore, thermogravimetric analysis curve of the phosphors reveals nearly no weight loss at the temperature below 160 °C (Figure S8). In liquid N_2, low-temperature stability of the phosphors is explored. The phosphors have nearly no variations in luminescent properties before and after treatment with liquid N_2 (Figure S9), demonstrating excellent resistance to low temperature. Besides, the phosphors exhibit good solvent resistance against organic solvents. As shown in Figure S10, the phosphors cannot be dissolved or swelled by chloroform even after being soaked for 1 week, and there are nearly no variations in their PL spectra during the period. Thus, the PL property is expected to be well-preserved when the phosphors are encapsulated into packaging materials for LEDs. To confirm this, mixtures of different colored QD-based phosphors and polydimethylsiloxane (PDMS) are solidified, and the temperature and duration for this solidification process are 80 °C and 1 h, respectively. The resultant strongly luminescent solid-state materials can be easily molded to different shapes (Figure S10d). The homogeneous emissions from the whole solid-state materials suggest a good distribution of the phosphors in PDMS, which is ascribed to the spherical structure and small size of phosphors (Figure 3d). To test the structural stability of the phosphors, we stretch the phosphor-filled elastic PDMS (Figure S11). PL emission is unchanged after stretching.

The microwave-assisted heating method is extendable to prepare phosphors from CdTe QDs decorated by other ligands, such as thioglycolic acid (TGA) and 1-thioglycerol (TG) (Figure S12). Furthermore, this method also permits the adoption of other QDs, such as MPA-modified CdSe and $CdSe_{0.25}Te_{0.75}$, to prepare phosphors (Figure S13). To sum up, the excellent photostability, thermal, solvent, mechanical stability, and high controllability of current QD-based phosphors ensure their potential applications as the color-conversion layer in LEDs.

First, the CdTe QD-based phosphors are blended with PDMS, and the mixtures are used to fill the void of LED chip. Then, the whole device is placed in an oven for solidification, where the temperature and duration for this solidification process is 80 °C and 1 h. By altering the emission of phosphors, LEDs with various emission colors are prepared (Figure 5). Figure 5f presents the CIE color coordinates of these LEDs, where the peripheral four points are (0.66, 0.27), (0.46, 0.48), (0.22, 0.46), and (0.14, 0.04). According to colorimetry, the LED emission colors in the four-points-encircled area can be easily regulated by utilizing different emissive phosphors. The relationship between CCT and CIE color coordinates can be concluded as the black curve in Figure 5f. On the basis of the area of the quadrangle, it is found that the CCT of the device can be adjusted from 1500 K to infinity, covering almost all CCT on earth. In addition, compared to QD aqueous solution, LEDs possess narrower fwhm (Figure 5a–e and Table 1), signifying a high-color purity of LEDs emission. As explained in detail before, the main reason for emission narrowing could be ascribed to reabsorption of QD emission.[51,65] Several simple WLEDs

DOI: 10.1021/acsami.8b06323
ACS Appl. Mater. Interfaces 2018, 10, 27160–27170

with different CCT are also obtained by combining the yellow emissive phosphors and the LEDs chips (Figure 6). Cool, pure, and warm WLEDs can be fabricated by tuning the mass ratio of the phosphors in the color conversion layer (Figure 6d), where the mass ratios are 1:25, 1:20, and 1:15 in cool, pure, and warm WLEDs, respectively. Although these WLEDs possess bright emissions, high-performance WLEDs, which can be used for tricolor display and high CRI illumination, are much desired.

To realize the high-performance WLEDs, the color-conversion layer should be composed of multiple QD-based phosphors with different emission colors, whereas it has a major concern about fluorescent resonance energy transfer (FRET) when directly mixing several different-sized QDs.[66] Meaningfully, because the QDs are confined in the phosphors, FRET is expected to be limited. To prove this, two different emissive phosphors with emission centered at 527 and 653 nm are employed because the green-emissive phosphors have no emission at the wavelength of 653 nm and vice versa (Figure 7a). After directly mixing these two phosphors, the PL

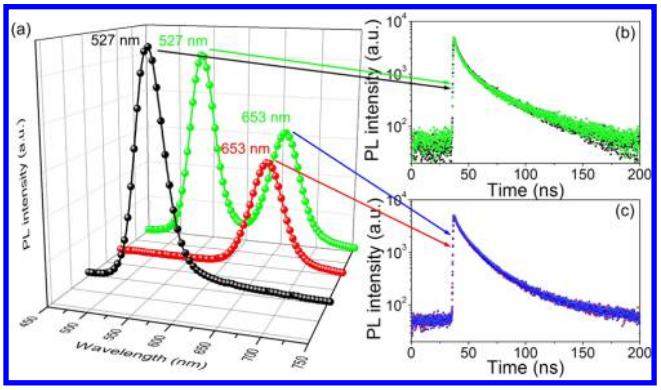

Figure 7. (a) PL spectra of CdTe QD-based phosphors with emissions centered at 527 nm (black), 653 nm (red), and their mixture (green). (b,c) PL decay curves of these phosphors measured at 527 (black and green) and 653 (red and blue) nm.

spectrum of the mixture presents two obviously distinct emission peaks, which are well-consistent with those of the initial phosphors (Figure 7a). The PL decay curves of the mixture are measured at 527 and 653 nm under 375 nm excitation (Figure 7b,c). By comparing with the PL decay curves of initial green/red emissive phosphors, no variations in the fluorescence lifetime (11.3 ns for green and 13.0 ns for red) are observed, indicating no FRET between these two phosphors, which is very beneficial to the realization of high-performance WLEDs.[67]

By utilizing the LED chip, 553 nm yellow emission and 671 nm red emission of the CdTe QD-based phosphors, a WLED with tricolor emission is fabricated (Figure 8a,b), where the phosphors with red emission are first deposited on the InGaN chip to prevent the reabsorption of green emission by the 671 nm phosphors, leading to the enhancement of their emitting efficiency (the inset of Figure 8c). The CIE coordinate of this tricolor WLEDs is (0.33, 0.33), indicating a pure white emission (Figure 8c). As shown in Figure 8b, these three peaks possess small fwhm less than 35 nm, indicating a potential application in back-light display.[19] Through depositing more kinds of phosphors with different emissions on the InGaN chip, a WLED with CRI of 90.3 is achieved (Figure 8d,e). Emissive peaks of these phosphors used in the WLED are centered at 520, 561, 590, 622, and 653 nm, and they are deposited successively on the InGaN chip in sequence from 653 to 520 nm (the inset of Figure 8f), which could avoid the emission reabsorption. Before evaluating the color-rendering property, an area light is fabricated by composing nine WLED devices to diminish local overexposure of point light source (Figures 8d and S14). Afterward, we compare the appearance color of several varicolored pen caps under the area light and sunlight, and there are nearly no differences under these two light sources (Figures 8d and S15), demonstrating the good color-rendering property. The CIE coordinate, CCT, and luminous efficacy of WLEDs is (0.35, 0.33), 4710 K, and 38 lm/W (Figure 8f), respectively. These parameters are comparable to those values of WLEDs in the previous reports,[16,61] and a WLED prototype is capable of illuminating a piece of A4 (Figure S16), demonstrating the strong luminous intensity of the WLEDs. Meanwhile, the luminous intensity of these WLEDs has no variation after several weeks continuous work, showing the significance of the phosphors in developing solid-state lighting (Figure S17). On the basis of these advantages of the QD-based phosphors in LEDs, a VLC device is built by using these phosphors as the color-conversion materials. A small-signal frequency−response measurement is carried out, and Figure 8g presents the sketch of the experimental apparatus. A bias-tee is used to supply power for the blue-emitting micro-LED (μLED), which can excite the phosphors, and then the resultant white light is converted into electrical signal by the avalanche photodiode (APD) photodetector. To catch the signal of this system, the modulation frequency is varied from 10 to 500 MHz, and the comparison between the transmitted data and the received data is monitored. Figure 8h shows frequency response of the light from the phosphors and the output white light, where the horizontal dash line represents −3 dB characteristics. By removing the blue light from the μLED utilizing a 495 nm long-pass optical filter, the light of the phosphors possesses a high bandwidth of 25 MHz at a current of 80 mA. This value is higher than 12.4 MHz of commercial nitride-based materials and 3−12 MHz of commercial $Y_3Al_5O_{12}$-based materials.[14] More meaningfully, the bandwidth of the white emission of this VLC device could achieve 42 MHz at a current of 80 mA (Table S1), suggesting nearly a fourfold enhancement than commercial rare-earth phosphors. Besides, the bandwidth comparisons with similar QD-based VLC devices are also performed. As reported in a recent literature,[18] CdSe/ZnS QDs were used for the LED-based VLC, where all of the bandwidth of three kinds of CdSe/ZnS QDs are below 3 MHz. In another report,[68] the bandwidth of QD converters in the QD-based VLC is also below 22 MHz. Furthermore, according to another paper,[69] the bandwidth of the white light from the QD-based VLC is only 19.7 MHz. Although the bandwidth of perovskite QD-based VLC can reach 73 MHz,[8] the high preparation cost and structural instability of perovskite QDs are still a main concern. Meanwhile, in our recently published paper,[70] the achievable bandwidth of carbon dot-based VLC device is up to 285 MHz. However, the PLQY of the carbon dot-based phosphors is only 25%, which is much lower than that of CdTe QD-based phosphors (69%). The broad emission spectrum of carbon dots hardly permits the production of WLEDs with high color purity. Besides, carbon dots only possess green emission, which leads to a low CRI value of WLEDs (79) and cannot meet the request of practical applications. All of the above studies suggest a bright

DOI: 10.1021/acsami.8b06323
ACS Appl. Mater. Interfaces 2018, 10, 27160−27170

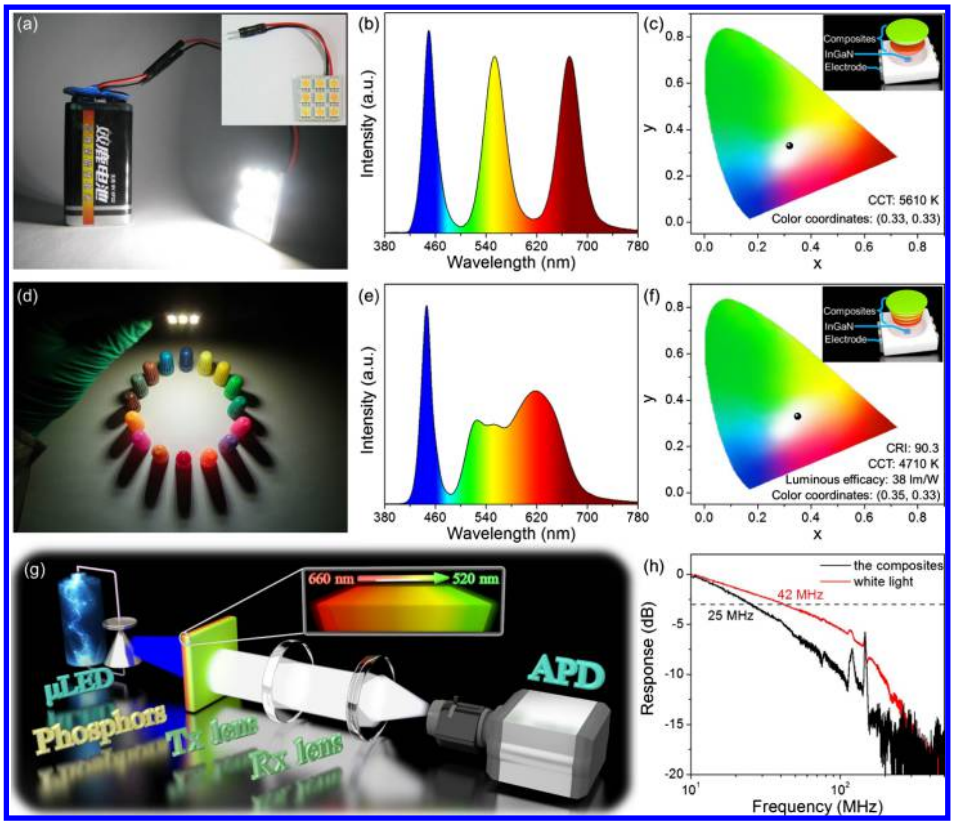

Figure 8. (a) Photograph of WLEDs area light source with tricolor emission. (b) Corresponding emission spectrum and (c) CIE color coordinate of the WLEDs are also shown. Inset of (c) is the depositional mode of the phosphors on the InGaN chip. (d) Photograph of WLEDs area light source with CRI of 90.3. (e) Corresponding emission spectrum and (f) CIE color coordinate of the WLEDs. The different-colored pen colors are used to evaluate the color-rendering property. Inset of (f) is the depositional mode of the phosphors on the InGaN chip. (g) Schematic diagram of the small-signal frequency−response measurement setup. (h) Plot of attenuation vs frequency of small-signal modulation. The dotted line corresponds to the −3 dB level which defines the bandwidth of the system.

application prospect of the QD-based phosphors reported here for various practical applications based on solid-state lighting.

CONCLUSIONS

In conclusion, a microwave-assisted heating method is developed for the fabrication of QD-based phosphors through microwaving the mixture of QDs and sodium silicate aqueous solution within only 30 s. Detailed investigations demonstrate that the resultant QD-based phosphors possess narrow fwhm, controllable composition, and tunable PL emission. Significantly, they display more than twice the enhancement in PLQYs (69%) compared with the initial QD aqueous solutions (33%), which can be ascribed to the variation of the refractive index around QDs and the QD surface optimization. Owing to the protection from the cross-linked structure, the QD-based phosphors also show good stability. These advantages permit the production of WLEDs with high color purity, controllable CCT, and high CRI (90.3), using the QD-based phosphors as color-conversion materials. Furthermore, luminescence lifetimes of the QD-based phosphors are less than 25 ns, which permit to fabricate a VLC device with a modulation bandwidth of 42 MHz.

METHODS

Materials. Tellurium powder (~200 mesh, 99.8%), TGA (98%), selenium powder (~100 mesh, ≥99.5%), TG (98%), and MPA (99+%) were obtained from Aldrich. Cadmium chloride (99%), $N_2H_4·H_2O$ (80%), sodium hydroxide (98%), 2-propanol, $Na_2SiO_3·9H_2O$ (Baume degree is 40), $NaBH_4$ (96%), and Na_2TeO_3 (98+%) were purchased from Aladdin and used without purification. Polydimethylsiloxane, referred to as PDMS, was obtained from Dow Corning. Millipore equipment was adopted to produce deionized water.

Room-Temperature Synthesis of MPA-, TGA-, and TG-Stabilized CdTe, CdSe, and $CdSe_{0.25}Te_{0.75}$ QDs Aqueous Solutions. CdTe QDs decorated by MPA were prepared based on our previous paper.[59] Briefly, 6 mL of cadmium chloride solution (100 mM), 93 mL of H_2O, 0.127 mL of MPA, 6 mL of sodium tellurite solution (20 mM), 50 mg of sodium borohydride, and 15 mL of hydrazine were poured into a bottle in sequence. The resultant QD concentration was 5×10^{-3} M with reference to cadmium ions. After adding the reagents in one pot, the QD solution was stored at room temperature in air under atmospheric pressure. By altering the storage durations from 1, 3, 8, 16 to 30 h, QDs with emissions of 520, 560, 590, 620, and 660 nm were formed. To terminate the QDs growth, 2-propanol was added into QD solution to remove $N_2H_4·H_2O$, and the mixture solution was centrifuged. Afterward, the resultant precipitates are dissolved in aqueous solution for further use. The aqueous solution contains cadmium chloride and MPA, and its pH is adjusted to 9.5 before use. Through an analogous process, CdTe QDs decorated by TG and TGA could also be synthesized except using TGA and TG as the capping ligand. Similarly, by using NaHSe/$NaHSe_{0.25}Te_{0.75}$ instead of TeO_3^{2-}, MPA-decorated aqueous CdSe and $CdSe_{0.25}Te_{0.75}$ QDs were fabricated.

Preparation of QD-Based Luminescent Phosphors in 30 s. Two millilitres of $Na_2SiO_3·9H_2O$ (Baume degree is 40) and 2 mL of CdTe QDs decorated by MPA (10 mM) were poured into a beaker. After microwaving this homogeneous solution for 30 s, a swollen solid foam with strong luminescence was formed. By altering the emission

DOI: 10.1021/acsami.8b06323
ACS Appl. Mater. Interfaces 2018, 10, 27160−27170

color and compositions of QDs, highly luminescent phosphors with emission peaks from 520 to 660 nm were obtained.

LED Packaging with QD-Based Phosphors. Unpacked InGaN LED chip with blue emission of 450 nm was adopted in the experiments. First, the QD-based luminescent phosphors were blended with PDMS precursor and poured into hollow space of the chips. After that, LEDs with different emission colors were achieved through solidifying them at 80 degree centigrade for 1 h.

Characterization. PL data were gathered using a Hitachi F-7000 apparatus. A Shimadzu UV-3101PC spectrophotometer was used to obtain UV−visible absorption data. An FLS920 spectrometer equipped with a calibrated integrating sphere was adopted to collect the absolute PLQYs of solution and phosphors. The measurement of PL decay profiles was realized through a specialized equipment called as LifeSpec-II manufactured by Edinburgh. Ultrafast TA spectroscopy and optical pumping investigations were carried out using a Ti:sapphire laser (Spectra-Physics, Spitfire ACE). Pump source at 400 nm was produced in a BBO crystal through frequency doubling of the 800 nm laser. A Fiber Optic spectrometer (Ocean Optics Maya2000 Pro) was applied to collect the spectrum. Thermogravimetric curves were read through an analyzer, and the instrument model was TA Q500. TEM and HRTEM analyses were carried out using a Tecnai-G2-F20 TEM. D5005 diffractometer produced by Siemens was used to measure X-ray powder diffraction patterns. SEM picture was taken employing electronic microscopy (JEOL FESEM 6700F), and the acceleration voltage is 3 kV. EDS was recorded on an Inca X-Max instrument. Nikon microscopy apparatus was applied to take the PL images of the powders. The characteristics of the LEDs were performed in an integrating sphere, and the signal was analyzed using the PR-650 equipment (Spectrascan, USA). A small-signal frequency−response measurement was performed to investigate the modulation bandwidth of the phosphors-converted light. A bias-tee combined with the electricity of Yokogawa GS610 is used to supply power for the blue-emitting μLED, which can excite the phosphors. The small signal was from an analyzer, and the instrument model was Agilent N5225A. A transmitter (Tx) mirror and a receiver (Rx) mirror were used to import the light into an analyzer (APD12702, 100 MHz).

■ ASSOCIATED CONTENT

Supporting Information

The Supporting Information is available free of charge on the ACS Publications website at DOI: 10.1021/acsami.8b06323.

Characterizations of CdTe QD aqueous solutions, illustration of the dehydration process of sodium silicate aqueous solutions, stabilities of the phosphors, and additional information of LEDs (PDF)

■ AUTHOR INFORMATION

Corresponding Authors

*E-mail: xiaoweixu@jlu.edu.cn (X.X.).
*E-mail: rqguo@fudan.edu.cn (R.Q.).
*E-mail: qusn@ciomp.ac.cn (S.Q.).
*E-mail: hao_zhang@jlu.edu.cn. Fax: +86 431 85193423 (H.Z.).

ORCID

Pengfei Tian: 0000-0001-8479-2727
Ruiqian Guo: 0000-0002-0498-0363
Songnan Qu: 0000-0003-4159-096X
Hao Zhang: 0000-0002-2373-1100

Author Contributions

The manuscript was written through contributions of all authors. All authors have given approval to the final version of the manuscript.

Notes

The authors declare no competing financial interest.

■ ACKNOWLEDGMENTS

This work was supported by the National Natural Science Foundation of China (projects nos. 51602304, 81600879, and 61675049), National Key Research and Development Program of China (2016YFB0401701), Jilin Province Science and Technology Research (projects nos. 20160520008JH, 20150519003JH, 20170101191JC, and 20170101042JC), China Postdoctoral Science Foundation (projects nos. 2018T110259 and 2016M601386), Fudan University-CIOMP Joint Fund (FC2017-004), and JLU Science and Technology Innovative Research Team (projects no. 2017TD-11).

■ REFERENCES

(1) Grandjean, N.; Butté, R. Solid-State Lighting on Glass. *Nat. Photonics* **2011**, *5*, 714−715.
(2) Aharonovich, I.; Englund, D.; Toth, M. Solid-State Single-Photon Emitters. *Nat. Photonics* **2016**, *10*, 631−641.
(3) Huang, X. Red Phosphor Converts White LEDs. *Nat. Photonics* **2014**, *8*, 748−749.
(4) Pust, P.; Weiler, V.; Hecht, C.; Tücks, A.; Wochnik, A. S.; Henß, A.-K.; Wiechert, D.; Scheu, C.; Schmidt, P. J.; Schnick, W. Narrow-band red-emitting Sr[LiAl 3 N 4]:Eu2+ as a next-generation LED-phosphor material. *Nat. Mater.* **2014**, *13*, 891−896.
(5) Pathak, P. H.; Feng, X.; Hu, P.; Mohapatra, P. Visible Light Communication, Networking, and Sensing: A Survey, Potential and Challenges. *IEEE Commun. Surv. Tutor.* **2015**, *17*, 2047−2077.
(6) Komine, T.; Nakagawa, M. Integrated System of White LED Visible-Light Communication and Power-Line Communication. *IEEE T. Consum. Electr.* **2003**, *49*, 71−79.
(7) Sajjad, M. T.; Manousiadis, P. P.; Chun, H.; Vithanage, D. A.; Rajbhandari, S.; Kanibolotsky, A. L.; Faulkner, G.; O'Brien, D.; Skabara, P. J.; Samuel, I. D. W.; Turnbull, G. A. Novel Fast Color-Converter for Visible Light Communication Using a Blend of Conjugated Polymers. *ACS Photonics* **2015**, *2*, 194−199.
(8) Mei, S.; Liu, X.; Zhang, W.; Liu, R.; Zheng, L.; Guo, R.; Tian, P. High-Bandwidth White-Light System Combining a Micro-LED with Perovskite Quantum Dots for Visible Light Communication. *ACS Appl. Mater. Interfaces* **2018**, *10*, 5641−5648.
(9) Dursun, I.; Shen, C.; Parida, M. R.; Pan, J.; Sarmah, S. P.; Priante, D.; Alyami, N.; Liu, J.; Saidaminov, M. I.; Alias, M. S.; Abdelhady, A. L.; Ng, T. K.; Mohammed, O. F.; Ooi, B. S.; Bakr, O. M. Perovskite Nanocrystals as a Color Converter for Visible Light Communication. *ACS Photonics* **2016**, *3*, 1150−1156.
(10) Lee, C.; Shen, C.; Oubei, H. M.; Cantore, M.; Janjua, B.; Ng, T. K.; Farrell, R. M.; El-Desouki, M. M.; Speck, J. S.; Nakamura, S.; Ooi, B. S.; DenBaars, S. P. 2 Gbit/s Data Transmission from an Unfiltered Laser-Based Phosphor-Converted White Lighting Communication System. *Opt. Express* **2015**, *23*, 29779−29787.
(11) Dai, P.-P.; Li, C.; Zhang, X.-T.; Xu, J.; Chen, X.; Wang, X.-L.; Jia, Y.; Wang, X.; Liu, Y.-C. A single Eu2+-activated high-color-rendering oxychloride white-light phosphor for white-light-emitting diodes. *Light: Sci. Appl.* **2016**, *5*, e16024.
(12) Li, X.; Budai, J. D.; Liu, F.; Howe, J. Y.; Zhang, J.; Wang, X.-J.; Gu, Z.; Sun, C.; Meltzer, R. S.; Pan, Z. New yellow Ba0.93Eu0.07Al2O4 phosphor for warm-white light-emitting diodes through single-emitting-center conversion. *Light: Sci. Appl.* **2013**, *2*, e50.
(13) Wang, L.; Xie, R.-J.; Li, Y.; Wang, X.; Ma, C.-G.; Luo, D.; Takeda, T.; Tsai, Y.-T.; Liu, R.-S.; Hirosaki, N. Ca1−xLi x Al1− x Si1+xN3:Eu2+ solid solutions as broadband, color-tunable and thermally robust red phosphors for superior color rendition white light-emitting diodes. *Light: Sci. Appl.* **2016**, *5*, e16155.
(14) O'Brien, D. C.; Zeng, L.; Le-Minh, H.; Faulkner, G.; Walewski, J. W.; Randel, S. Visible light communications: Challenges and

DOI: 10.1021/acsami.8b06323
ACS Appl. Mater. Interfaces 2018, 10, 27160−27170

possibilities. *Personal, Indoor and Mobile Radio Communications, (PIMRC 2008), IEEE 19th International Symposium*, 2008; pp 1−5.
(15) Dai, Q.; Duty, C. E.; Hu, M. Z. Semiconductor-Nanocrystals-Based White Light-Emitting Diodes. *Small* **2010**, *6*, 1577−1588.
(16) Zhou, D.; Liu, M.; Lin, M.; Bu, X.; Luo, X.; Zhang, H.; Yang, B. Hydrazine-Mediated Construction of Nanocrystal Self-Assembly Materials. *ACS Nano* **2014**, *8*, 10569−10581.
(17) Jang, E.; Jun, S.; Jang, H.; Lim, J.; Kim, B.; Kim, Y. White-Light-Emitting Diodes with Quantum Dot Color Converters for Display Backlights. *Adv. Mater.* **2010**, *22*, 3076−3080.
(18) Xiao, X.; Tang, H.; Zhang, T.; Chen, W.; Chen, W.; Wu, D.; Wang, R.; Wang, K. Improving the Modulation Bandwidth of LED by CdSe/ZnS Quantum Dots for Visible Light Communication. *Opt. Express* **2016**, *24*, 21577−21586.
(19) Abe, S.; Joos, J. J.; Martin, L. I. D. J.; Hens, Z.; Smet, P. F. Hybrid Remote Quantum Dot/Powder Phosphor Designs for Display Backlights. *Light: Sci. Appl.* **2017**, *6*, e16271.
(20) Adam, M.; Gaponik, N.; Eychmüller, A.; Erdem, T.; Soran-Erdem, Z.; Demir, H. V. Colloidal Nanocrystals Embedded in Macrocrystals: Methods and Applications. *J. Phys. Chem. Lett.* **2016**, *7*, 4117−4123.
(21) Zhu, M.; Peng, X.; Wang, Z.; Bai, Z.; Chen, B.; Wang, Y.; Hao, H.; Shao, Z.; Zhong, H. Highly Transparent and Colour-Tunable Composite Films with Increased Quantum Dot Loading. *J. Mater. Chem. C* **2014**, *2*, 10031−10036.
(22) Dai, X.; Zhang, Z.; Jin, Y.; Niu, Y.; Cao, H.; Liang, X.; Chen, L.; Wang, J.; Peng, X. Solution-Processed, High-Performance Light-Emitting Diodes Based on Quantum Dots. *Nature* **2014**, *515*, 96−99.
(23) Kim, S.; Kim, T.; Kang, M.; Kwak, S. K.; Yoo, T. W.; Park, L. S.; Yang, I.; Hwang, S.; Lee, J. E.; Kim, S. K.; Kim, S.-W. Highly Luminescent InP/GaP/ZnS Nanocrystals and Their Application to White Light-Emitting Diodes. *J. Am. Chem. Soc.* **2012**, *134*, 3804−3809.
(24) Gaponik, N.; Talapin, D. V.; Rogach, A. L.; Hoppe, K.; Shevchenko, E. V.; Kornowski, A.; Eychmüller, A.; Weller, H. Thiol-Capping of CdTe Nanocrystals: An Alternative to Organometallic Synthetic Routes. *J. Phys. Chem. B* **2002**, *106*, 7177−7185.
(25) Shi, L.; Zhu, L.; Guo, J.; Zhang, L.; Shi, Y.; Zhang, Y.; Hou, K.; Zheng, Y.; Zhu, Y.; Lv, J.; Liu, S.; Tang, Z. Self-Assembly of Chiral Gold Clusters into Crystalline Nanocubes of Exceptional Optical Activity. *Angew. Chem., Int. Ed.* **2017**, *56*, 15397−15401.
(26) Zhou, Y.; Zhu, Z.; Huang, W.; Liu, W.; Wu, S.; Liu, X.; Gao, Y.; Zhang, W.; Tang, Z. Optical Coupling between Chiral Biomolecules and Semiconductor Nanoparticles: Size-Dependent Circular Dichroism Absorption. *Angew. Chem., Int. Ed.* **2011**, *50*, 11456−11459.
(27) Gao, X.; Zhang, X.; Deng, K.; Han, B.; Zhao, L.; Wu, M.; Shi, L.; Lv, J.; Tang, Z. Excitonic Circular Dichroism of Chiral Quantum Rods. *J. Am. Chem. Soc.* **2017**, *139*, 8734−8739.
(28) Qin, B.; Chen, H.; Liang, H.; Fu, L.; Liu, X.; Qiu, X.; Liu, S.; Song, R.; Tang, Z. Reversible Photoswitchable Fluorescence in Thin Films of Inorganic Nanoparticle and Polyoxometalate Assemblies. *J. Am. Chem. Soc.* **2010**, *132*, 2886−2888.
(29) Li, Z.; Zhu, Z.; Liu, W.; Zhou, Y.; Han, B.; Gao, Y.; Tang, Z. Reversible Plasmonic Circular Dichroism of Au Nanorod and DNA Assemblies. *J. Am. Chem. Soc.* **2012**, *134*, 3322−3325.
(30) Adam, M.; Wang, Z.; Dubavik, A.; Stachowski, G. M.; Meerbach, C.; Soran-Erdem, Z.; Rengers, C.; Demir, H. V.; Gaponik, N.; Eychmüller, A. Liquid-Liquid Diffusion-Assisted Crystallization: A Fast and Versatile Approach Toward High Quality Mixed Quantum Dot-Salt Crystals. *Adv. Funct. Mater.* **2015**, *25*, 2638−2645.
(31) Shen, H.; Cao, W.; Shewmon, N. T.; Yang, C.; Li, L. S.; Xue, J. High-Efficiency, Low Turn-on Voltage Blue-Violet Quantum-Dot-Based Light-Emitting Diodes. *Nano Lett.* **2015**, *15*, 1211−1216.
(32) Kim, B. H.; Onses, M. S.; Lim, J. B.; Nam, S.; Oh, N.; Kim, H.; Yu, K. J.; Lee, J. W.; Kim, J.-H.; Kang, S.-K.; Lee, C. H.; Lee, J.; Shin, J. H.; Kim, N. H.; Leal, C.; Shim, M.; Rogers, J. A. High-Resolution Patterns of Quantum Dots Formed by Electrohydrodynamic Jet Printing for Light-Emitting Diodes. *Nano Lett.* **2015**, *15*, 969−973.
(33) Wang, X.; Yan, X.; Li, W.; Sun, K. Doped Quantum Dots for White-Light-Emitting Diodes Without Reabsorption of Multiphase Phosphors. *Adv. Mater.* **2012**, *24*, 2742−2747.
(34) He, Y.; Sai, L.-M.; Lu, H.-T.; Hu, M.; Lai, W.-Y.; Fan, Q.-L.; Wang, L.-H.; Huang, W. Microwave-Assisted Synthesis of Water-Dispersed CdTe Nanocrystals with High Luminescent Efficiency and Narrow Size Distribution. *Chem. Mater.* **2007**, *19*, 359−365.
(35) Bao, H.; Wang, E.; Dong, S. One-Pot Synthesis of CdTe Nanocrystals and Shape Control of Luminescent CdTe-Cystine Nanocomposites. *Small* **2006**, *2*, 476−480.
(36) Guo, J.; Yang, W.; Wang, C. Systematic Study of the Photoluminescence Dependence of Thiol-Capped CdTe Nanocrystals on the Reaction Conditions. *J. Phys. Chem. B* **2005**, *109*, 17467−17473.
(37) Otto, T.; Müller, M.; Mundra, P.; Lesnyak, V.; Demir, H. V.; Gaponik, N.; Eychmüller, A. Colloidal Nanocrystals Embedded in Macrocrystals: Robustness, Photostability, and Color Purity. *Nano Lett.* **2012**, *12*, 5348−5354.
(38) Kalytchuk, S.; Zhovtiuk, O.; Rogach, A. L. Sodium Chloride Protected CdTe Quantum Dot Based Solid-State Luminophores with High Color Quality and Fluorescence Efficiency. *Appl. Phys. Lett.* **2013**, *103*, 103105.
(39) Jun, S.; Lee, J.; Jang, E. Highly Luminescent and Photostable Quantum Dot-Silica Monolith and Its Application to Light-Emitting Diodes. *ACS Nano* **2013**, *7*, 1472−1477.
(40) Zorn, M.; Bae, W. K.; Kwak, J.; Lee, H.; Lee, C.; Zentel, R.; Char, K. Quantum Dot−Block Copolymer Hybrids with Improved Properties and Their Application to Quantum Dot Light-Emitting Devices. *ACS Nano* **2009**, *3*, 1063−1068.
(41) Kim, K.; Woo, J. Y.; Jeong, S.; Han, C.-S. Photoenhancement of a Quantum Dot Nanocomposite via UV Annealing and its Application to White LEDs. *Adv. Mater.* **2011**, *23*, 911−914.
(42) Müller, M.; Kaiser, M.; Stachowski, G. M.; Resch-Genger, U.; Gaponik, N.; Eychmüller, A. Photoluminescence Quantum Yield and Matrix-Induced Luminescence Enhancement of Colloidal Quantum Dots Embedded in Ionic Crystals. *Chem. Mater.* **2014**, *26*, 3231−3237.
(43) Demir, H. V.; Nizamoglu, S.; Erdem, T.; Mutlugun, E.; Gaponik, N.; Eychmüller, A. Quantum Dot Integrated LEDs Using Photonic and Excitonic Color Conversion. *Nano Today* **2011**, *6*, 632−647.
(44) Ouyang, J.; Zaman, M. B.; Yan, F. J.; Johnston, D.; Li, G.; Wu, X.; Leek, D.; Ratcliffe, C. I.; Ripmeester, J. A.; Yu, K. Multiple Families of Magic-Sized CdSe Nanocrystals with Strong Bandgap Photoluminescence via Noninjection One-Pot Syntheses. *J. Phys. Chem. C* **2008**, *112*, 13805−13811.
(45) Zheng, Y.; Gao, S.; Ying, J. Y. Synthesis and Cell-Imaging Applications of Glutathione-Capped CdTe Quantum Dots. *Adv. Mater.* **2007**, *19*, 376−380.
(46) Bao, H.; Gong, Y.; Li, Z.; Gao, M. Enhancement Effect of Illumination on the Photoluminescence of Water-Soluble CdTe Nanocrystals: Toward Highly Fluorescent CdTe/CdS Core−Shell Structure. *Chem. Mater.* **2004**, *16*, 3853−3859.
(47) Yin, H.; Yi, J.; Yang, Z.-W.; Xu, Z.-Y.; Xie, S.-J.; Li, L.; Li, C.-Y.; Xu, J.; Zhang, H.; Zhang, S.-J.; Li, J.-F.; Tian, Z.-Q. Plasmon Enhanced Quantum Dots Fluorescence and Energy Conversion in Water Splitting Using Shell-Isolated Nanoparticles. *Nano Energy* **2017**, *42*, 232−240.
(48) Murray, C. B.; Norris, D. J.; Bawendi, M. G. Synthesis and characterization of nearly monodisperse CdE (E = sulfur, selenium, tellurium) semiconductor nanocrystallites. *J. Am. Chem. Soc.* **1993**, *115*, 8706−8715.
(49) Rajh, T.; Micic, O. I.; Nozik, A. J. Synthesis and characterization of surface-modified colloidal cadmium telluride quantum dots. *J. Phys. Chem.* **1993**, *97*, 11999−12003.
(50) Sun, C.; Zhang, Y.; Ruan, C.; Yin, C.; Wang, X.; Wang, Y.; Yu, W. W. Efficient and Stable White LEDs with Silica-Coated Inorganic Perovskite Quantum Dots. *Adv. Mater.* **2016**, *28*, 10088−10094.

DOI: 10.1021/acsami.8b06323
ACS Appl. Mater. Interfaces 2018, 10, 27160−27170

(51) Zhou, D.; Zou, H.; Liu, M.; Zhang, K.; Sheng, Y.; Cui, J.; Zhang, H.; Yang, B. Surface Ligand Dynamics-Guided Preparation of Quantum Dots-Cellulose Composites for Light-Emitting Diodes. *ACS Appl. Mater. Interfaces* **2015**, *7*, 15830−15839.
(52) Liang, R.; Yan, D.; Tian, R.; Yu, X.; Shi, W.; Li, C.; Wei, M.; Evans, D. G.; Duan, X. Quantum Dots-Based Flexible Films and Their Application as the Phosphor in White Light-Emitting Diodes. *Chem. Mater.* **2014**, *26*, 2595−2600.
(53) Selvan, S. T.; Patra, P. K.; Ang, C. Y.; Ying, J. Y. Synthesis of Silica-Coated Semiconductor and Magnetic Quantum Dots and Their Use in the Imaging of Live Cells. *Angew. Chem., Int. Ed.* **2007**, *46*, 2448−2452.
(54) Chan, Y.; Snee, P. T.; Caruge, J.-M.; Yen, B. K.; Nair, G. P.; Nocera, D. G.; Bawendi, M. G. A Solvent-Stable Nanocrystal-Silica Composite Laser. *J. Am. Chem. Soc.* **2006**, *128*, 3146−3147.
(55) Zhou, L.; Gao, C.; Hu, X.; Xu, W. One-Pot Large-Scale Synthesis of Robust Ultrafine Silica-Hybridized CdTe Quantum Dots. *ACS Appl. Mater. Interfaces* **2010**, *2*, 1211−1219.
(56) Lin, N.; Hu, F.; Sun, Y.; Wu, C.; Xu, H.; Liu, X. Y. Construction of White-Light-Emitting Silk Protein Hybrid Films by Molecular Recognized Assembly among Hierarchical Structures. *Adv. Funct. Mater.* **2014**, *24*, 5284−5290.
(57) Yang, P.; Zhao, Y.; Lu, Y.; Xu, Q.-Z.; Xu, X.-W.; Dong, L.; Yu, S.-H. Phenol Formaldehyde Resin Nanoparticles Loaded with CdTe Quantum Dots: A Fluorescence Resonance Energy Transfer Probe for Optical Visual Detection of Copper(II) Ions. *ACS Nano* **2011**, *5*, 2147−2154.
(58) Lee, J.; Sundar, V. C.; Heine, J. R.; Bawendi, M. G.; Jensen, K. F. Full Color Emission from II-VI Semiconductor Quantum Dot-Polymer Composites. *Adv. Mater.* **2000**, *12*, 1102−1105.
(59) Zhou, D.; Lin, M.; Chen, Z.; Sun, H.; Zhang, H.; Sun, H.; Yang, B. Simple Synthesis of Highly Luminescent Water-Soluble CdTe Quantum Dots with Controllable Surface Functionality. *Chem. Mater.* **2011**, *23*, 4857−4862.
(60) Li, Y.; Cheng, X.; Cao, W.; Gong, L.; Zhang, R.; Zhang, H. Fabrication of Adiabatic Foam at Low Temperature with Sodium Silicate as Raw Material. *Mater. Des.* **2015**, *88*, 1008−1014.
(61) Chang, Y.; Yao, X.; Zhang, Z.; Jiang, D.; Yu, Y.; Mi, L.; Wang, H.; Li, G.; Yu, D.; Jiang, Y. Preparation of highly luminescent BaSO4 protected CdTe quantum dots as conversion materials for excellent color-rendering white LEDs. *J. Mater. Chem. C* **2015**, *3*, 2831−2836.
(62) Wang, W.; Liu, B.; Wang, Y.; Zhang, Z.; Chen, Y.; Wei, L. Morphology control and photoluminescence of BaMgAl10O17:Eu2+, Mn2+ phosphors prepared by flux method. *Mater. Lett.* **2011**, *65*, 3580−3582.
(63) Lide, D. R. *Handbook of Chemistry and Physics*, 89th ed.; Taylor & Francis Group: Oxfordshire, U.K., 2008.
(64) Chhajed, S.; Lee, W.; Cho, J.; Schubert, E. F.; Kim, J. K. Strong Light Extraction Enhancement in GaInN Light-Emitting Diodes by Using Self-Organized Nanoscale Patterning of *p*-Type GaN. *Appl. Phys. Lett.* **2011**, *98*, 071102.
(65) Zhou, D.; Zhai, Y.; Qu, S.; Li, D.; Jing, P.; Ji, W.; Shen, D.; Rogach, A. L. Electrostatic Assembly Guided Synthesis of Highly Luminescent Carbon-Nanodots@BaSO4Hybrid Phosphors with Improved Stability. *Small* **2017**, *13*, 1602055.
(66) Clapp, A. R.; Medintz, I. L.; Mauro, J. M.; Fisher, B. R.; Bawendi, M. G.; Mattoussi, H. Fluorescence Resonance Energy Transfer Between Quantum Dot Donors and Dye-Labeled Protein Acceptors. *J. Am. Chem. Soc.* **2004**, *126*, 301−310.
(67) Crooker, S. A.; Hollingsworth, J. A.; Tretiak, S.; Klimov, V. I. Spectrally Resolved Dynamics of Energy Transfer in Quantum-Dot Assemblies: Towards Engineered Energy Flows in Artificial Materials. *Phys. Rev. Lett.* **2002**, *89*, 186802.
(68) Leitao, M. F.; Santos, J. M. M.; Guilhabert, B.; Watson, S.; Kelly, A. E.; Islim, M. S.; Haas, H.; Dawson, M. D.; Laurand, N. Gb/s Visible Light Communications with Colloidal Quantum Dot Color Converters. *IEEE J. Sel. Top. Quantum Electron.* **2017**, *23*, 1−10.
(69) Laurand, N.; Guilhabert, B.; McKendry, J.; Kelly, A. E.; Rae, B.; Massoubre, D.; Gong, Z.; Gu, E.; Henderson, R.; Dawson, M. D. Colloidal Quantum Dot Nanocomposites for Visible Wavelength Conversion of Modulated Optical Signals. *Opt. Mater. Express* **2012**, *2*, 250−260.
(70) Zhou, Z.; Tian, P.; Liu, X.; Mei, S.; Zhou, D.; Li, D.; Jing, P.; Zhang, W.; Guo, R.; Qu, S.; Rogach, A. L. Hydrogen Peroxide-Treated Carbon Dot Phosphor with a Bathochromic-Shifted, Aggregation-Enhanced Emission for Light-Emitting Devices and Visible Light Communication. *Adv. Sci.* **2018**, 1800369.

DOI: 10.1021/acsami.8b06323
ACS Appl. Mater. Interfaces 2018, 10, 27160−27170